J Wood Sci (2001) 47:262–268

ORIGINAL ARTICLE

Hiroshi Yoshihara · Shinji Oka

Measurement of bending properties of wood by compression bending tests

Received: March 29, 2000 / Accepted: August 9, 2000

Abstract We measured Young's modulus, proportional limit stress, and bending strength by the compression bending test and examined the applicability of the testing method by comparing it with conventional bending test methods. Long columns of todomatsu (Japanese fir, *Abies sachalinensis* Fr. Schmidt) with various length/thickness ratios were the specimens. A compressive load was axially applied to the specimen supported with pin ends. Young's modulus, the proportional limit stress, and the bending strength were obtained from the load–loading point displacement and load–strains at the outer surfaces until the occurrence of bending failure. Four-point bending tests were also conducted, and the bending properties obtained were compared with the corresponding properties obtained by the compression bending tests. Based on the experimental results, we believe that when the stress–strain relation is measured by the load–loading point displacement relation using specimens whose length/thickness ratio is large enough, the bending properties can be obtained properly using the compression bending test.

Key words Compression bending test · Young's modulus · Proportional limit stress · Bending strength

Introduction

Several previous studies on conventional bending test methods for wood suggest that the stress condition around the loading nose is distorted seriously, and that the bending properties are influenced by the loading condition.[1–3] We fear that the bending properties of wood cannot be evaluated properly by the conventional bending method because of the distorted stress condition.

H. Yoshihara (✉) · S. Oka
Faculty of Science and Engineering, Shimane University,
1060 Nishikawazu-cho, Matsue, Shimane 690-8504, Japan
Tel. +81-852-32-6508; Fax +81-852-32-6123
e-mail: yosihara@riko.shimane-u.ac.jp

A new bending method was recently developed by Fukuda and colleagues for advanced composites with strong orthotropy.[4–7] In their method, a compression load is applied along the long axis of the specimen with a rectangular cross section, and Young's modulus and the bending strength are measured by means of the elastica phenomenon. The materials examined in their studies were brittle, and they did not show the material's nonlinearity, which wood often shows in the large strain region.

Although we believe that Fukuda's method is promising for measuring the bending properties of wood, the bending behavior of wood during compression bending should be examined in detail. Hence we examined the applicability of the compression bending test method for evaluating the bending properties of wood by comparing it with conventional bending tests.

Theories

A rectangular bar of known length, breadth, and thickness (l, b, t) is supported with pin ends. When the axial load P is applied in the long axis, the bending moment M is derived as:[8]

$$M = P\delta \tag{1}$$

where δ is the deflection at the mid-span. The stress at the outer side of the mid-span σ_{bc} is:

$$\sigma_{bc} = \frac{6M}{bt^2} = \frac{6P\delta}{bt^2} \tag{2}$$

From Eq. (2), σ_{bc} can be derived when the deflection δ is measured. This deflection is derived by the loading point displacement or the strains at outer surfaces. When the loading point displaces x after bifurcation, x/l is derived by the following equation.

$$\frac{x}{l} = 2 - \frac{2E(p)}{K(p)} \tag{3}$$

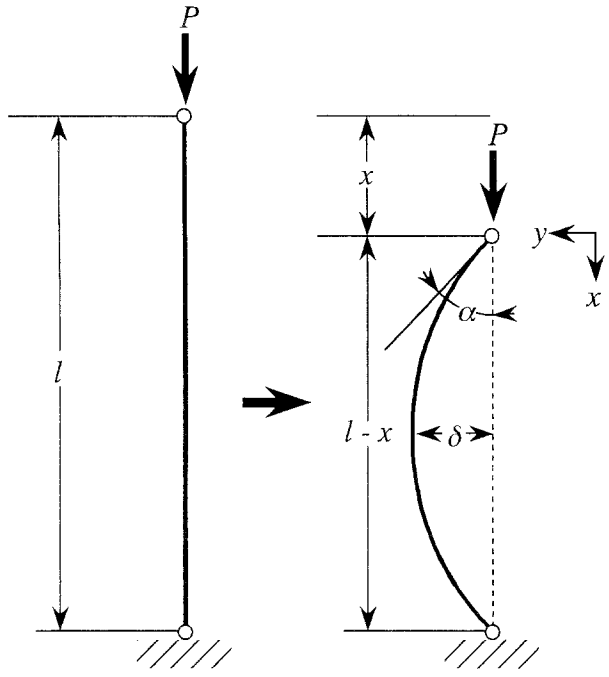

Fig. 1. Schematic diagram of compression bending

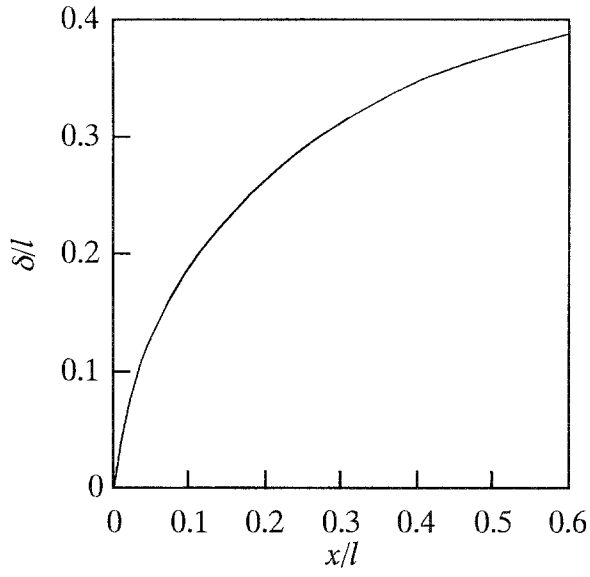

Fig. 2. δ/l–x/l relation. δ, l, and x are the deflection at the mid-span, length of specimen, and loading point displacement after bifurcation, respectively

where p is represented by the deflection angle at loading point α, which is shown in Fig. 1, as:

$$p = \sin\frac{\alpha}{2} \tag{4}$$

and $E(p)$ and $K(p)$ are given as:

$$E(p) = \int_0^{\frac{\pi}{2}} \sqrt{1 - p^2 \sin^2\phi}\, d\phi \tag{5}$$

and

$$K(p) = \int_0^{\frac{\pi}{2}} \frac{d\phi}{\sqrt{1 - p^2 \sin^2\phi}} \tag{6}$$

The mid-span deflection per length is derived as follows.

$$\frac{\delta}{l} = \frac{p}{K(p)} \tag{7}$$

From Eqs. (3) and (7), the δ/l–x/l relation can be derived by intervening the angle α, which is shown in Fig. 2. Thus, the deflection at the mid-span can be obtained from the loading point displacement. Another method for determining δ is to measure the strains at the outer planes. When the tensile and compressive strains at the outer planes are ε_t and ε_c, respectively, the radius of curvature at the mid-span is obtained as:

$$\rho = \frac{t}{\varepsilon_t - \varepsilon_c} \tag{8}$$

The radius of curvature can be also obtained by p and $K(p)$ as:

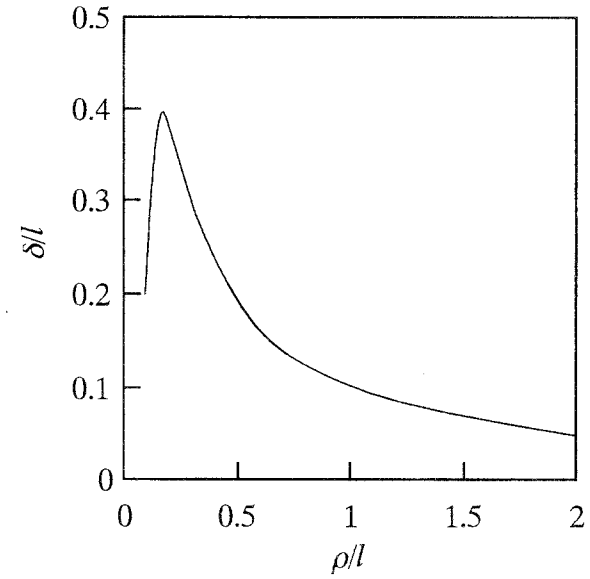

Fig. 3. The δ/l–ρ/l relation, where ρ is the radius of curvature at the mid-span

$$\frac{\rho}{l} = \frac{1}{4pK(p)} \tag{9}$$

From Eqs. (7) and (9), the δ/l–ρ/l relation, shown as Fig. 3, can be derived by intervening the angle α. Hence, δ is also derived by the strains at the outer planes.

Similarly, the longitudinal strain at the outer plane ε_{bc} is determined by the following two procedures. From Eqs. (3) and (9), the ρ/l–x/l relation is derived by intervening the angle α, as in Fig. 4. Then ε_{bc} is derived by the radius of curvature as:

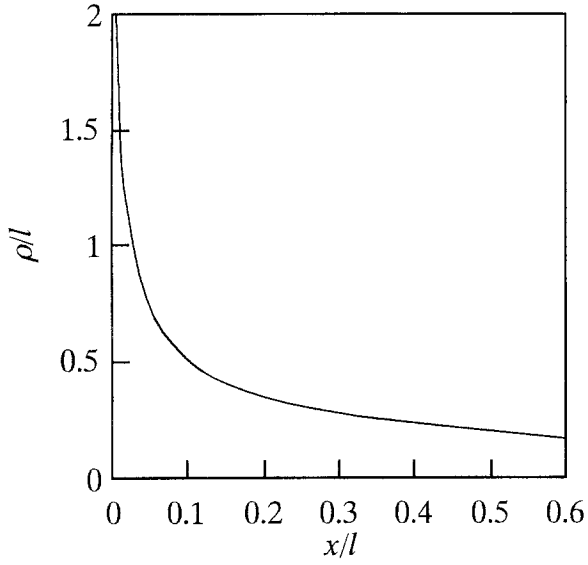

Fig. 4. The ρ/l–x/l relation

$$\varepsilon_{bc} = \frac{t}{2\rho} \tag{10}$$

Another method is to average the absolute values of tensile and compressive strains. By this method, ε_{bc} is derived as:

$$\varepsilon_{bc} = \frac{|\varepsilon_t| + |\varepsilon_c|}{2} = \frac{\varepsilon_t - \varepsilon_c}{2} \tag{11}$$

The σ_{bc}–ε_{bc} relation can be determined by these procedures.

Experiment

Materials

Todomatsu (a kind of Japanese fir, *Abies sachalinensis* Fr. Schmidt) whose density was 0.38 g/cm^3 was used for the specimens. All specimens were cut from lumber and were conditioned at 20°C and 65% relative humidity (RH) before and during the tests.

Compression bending tests

Column specimens were cut with the rectangular cross sections of 5, 10, and 15 mm (radial direction) × 25 mm (tangential direction). The lengths of the specimens varied from 200 to 500 mm at intervals of 100 mm. Strain gauges (gauge length 2 mm; Tokyo Sokki, Tokyo, Japan) were bonded at the center of the longitudinal-radial (LR) planes for measuring normal strains in the loading direction, ε_t and ε_c. Figure 5 shows the testing equipment used. This equipment consisted of V-notched and cylindrical attachments. Recently, Fukuda and Itabashi proposed a simple compression bending method.[7] They used a pair of shallow V-notched attachments by which both ends of a specimen were supported, and the load was directly applied by means of the

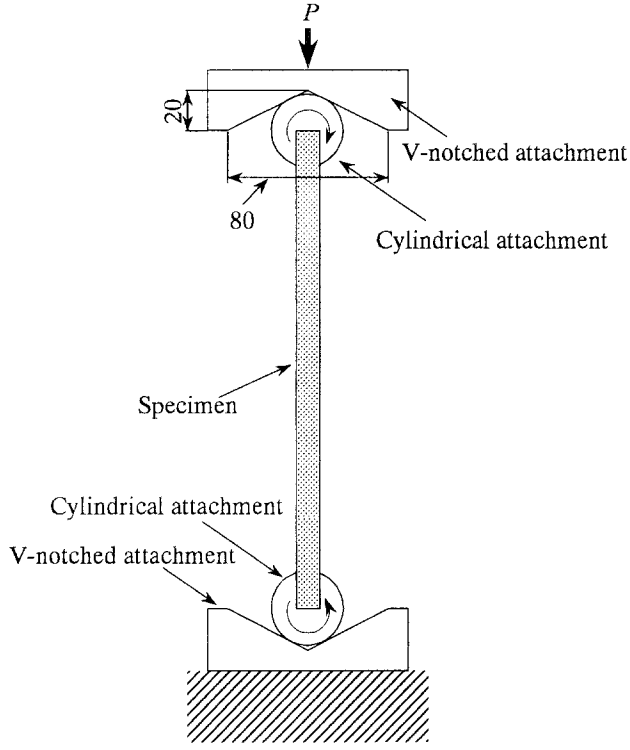

Fig. 5. Compression bending test equipment. Units are millimeters

attachments. Preliminarily, we tried to use their simple device, but the edges of the specimen seriously collapsed near the attachments and the pin-support condition could not be realized. To reduce this problem, the specimen whose sides were inserted into the grooves cut on the sides of cylindrical attachments was supported between the V notched attachments, as in Fig. 5. The load was applied by means of these attachments. To have the cylindrical attachments rotate freely in the V notches, Teflon sheets were placed between the cylindrical and V notched attachments. The load with a velocity of 2 mm/min was axially applied, and the loading point displacement was measured from the cross-head movement. Eight specimens were used in one test condition.

Figure 6 shows the load–loading point displacement relation. As in Fig. 6, the bifurcation point was determined as the start of nonlinear behavior, which is due to geometric nonlinearity and not material nonlinearity. This point coincided well with the blanching point of strains at both surfaces. The value of x was derived by subtracting the displacement before the bifurcation from the total displacement. Similarly, the value of l should have been essentially derived by subtracting the displacement before the bifurcation from the initial length. Nevertheless, we certified the displacement before the bifurcation had even a small influence on l, and the value of l was derived by the initial length. When determining the relations among δ/l, ρ/l, and x/l, it is inconvenient to refer to the diagrams or the tables showing these relations. Therefore, we approximated these relations by different power functions before and after $x/l = 0.1$, respectively, as follows:

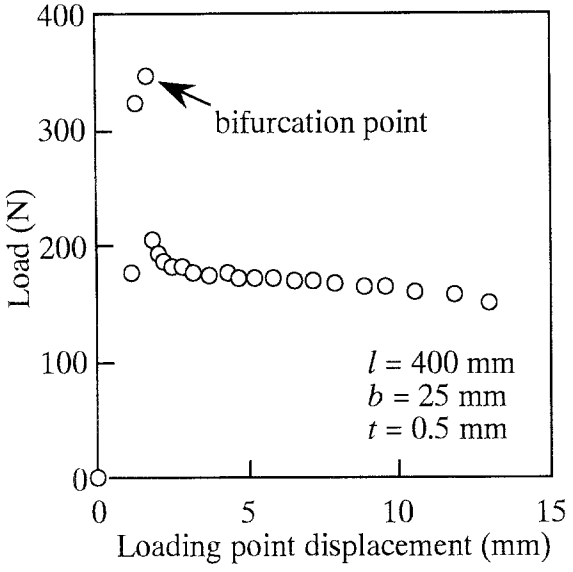

Fig. 6. Load–loading point displacement relation

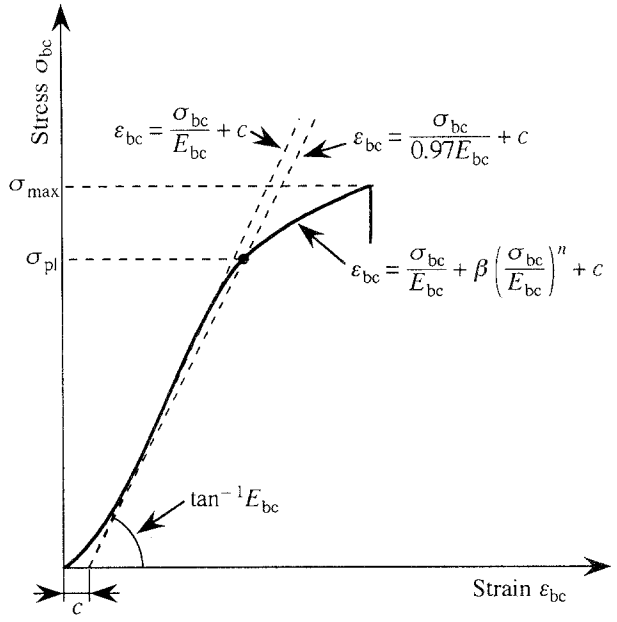

Fig. 7. Stress–strain diagram and the determination of parameters

$$\frac{\delta}{l} = \begin{cases} 0.620 \cdot \left(\dfrac{x}{l}\right)^{0.50} & \left(0 \le \dfrac{x}{l} < 0.1\right) \\ 0.505 \cdot \left(\dfrac{x}{l}\right)^{0.40} & \left(\dfrac{x}{l} \ge 0.1\right) \end{cases} \tag{12}$$

$$\frac{\rho}{l} = \begin{cases} 0.157 \cdot \left(\dfrac{x}{l}\right)^{-0.50} & \left(0 \le \dfrac{x}{l} < 0.1\right) \\ 0.138 \cdot \left(\dfrac{x}{l}\right)^{-0.56} & \left(\dfrac{x}{l} \ge 0.1\right) \end{cases} \tag{13}$$

As for the δ/l–ρ/l relation,

$$\frac{\delta}{l} = \begin{cases} 0.101 \cdot \left(\dfrac{\rho}{l}\right)^{-0.86} & \left(0 \le \dfrac{\rho}{l} < 0.5\right) \\ 0.100 \cdot \left(\dfrac{\rho}{l}\right)^{-1.00} & \left(\dfrac{\rho}{l} \ge 0.5\right) \end{cases} \tag{14}$$

where $\rho/l = 0.5$ corresponds approximately to $x/l = 0.1$. From the relations among x/l, δ/l, and ρ/l, the stress (σ_{bc})–strain (ε_{bc}) relation was obtained by the procedure mentioned above. This σ_{bc}–ε_{bc} relation was regressed into Ramberg-Osgood's power function, expressed as follows.[9]

$$\varepsilon_{bc} = \frac{\sigma_{bc}}{E_{bc}} + \beta\left(\frac{\sigma_{bc}}{E_{bc}}\right)^n + c \tag{15}$$

where E_{bc} is Young's modulus, c is the offset strain, and β and n are the material parameters. The proportional limit stress σ_{pl} (3% proportional limit stress) was determined as the intersection point of Eq. (15) and the straight line, represented as:

$$\varepsilon_{bc} = \frac{\sigma_{bc}}{0.97E_{bc}} + c \tag{16}$$

Hence, σ_{pl} is calculated as:

$$\sigma_{pl} = E_{bc}\left(\frac{3}{97\beta}\right)^{\frac{1}{n-1}} \tag{17}$$

The bending strength σ_{max} was derived by the maximum stress. Figure 7 shows the method for determining E_{bc}, σ_{pl}, and σ_{max}.

Four-point bending tests

Young's modulus, the proportional limit stress, and the bending strength were independently measured by the conventional four-point bending tests. These values were compared with those obtained by the compression bending tests.

The dimensions of the specimen were 15 mm in width, 15 mm in thickness, and 600 mm in length. The specimen was supported by a span of 450 mm, and the load was vertically applied at the trisected points of the span by loading noses, whose radii were 30 mm. The loading velocity was 5 mm/min, and the deflection at the center of the specimen was measured by a dial gauge placed below the specimen. The load–deflection relation was regressed into Ramberg-Osgood's power function written similarly to Eq. (15). The initial inclination of the load–deflection diagram $\Delta P/\Delta y$, 3% proportional limit load (P_{bp}), and load at the occurrence of breakage (P_{bt}) were obtained. In this case, $\Delta P/\Delta y$ and P_{bp} correspond to E_{bc} and σ_{pl}, respectively, in Eq. (15). Young's modulus E_{bt}, proportional limit stress σ_{bp}, and bending strength σ_{bt} were calculated using the equations based on the elementary bending theory as:

$$E_{bt} = \frac{23L^3}{108wh^3} \cdot \frac{\Delta P}{\Delta y} \tag{18}$$

$$\sigma_{bp} = \frac{P_{bp}L}{wh^2} \tag{19}$$

and

$$\sigma_{bt} = \frac{P_{bt}L}{wh^2} \tag{20}$$

where L, w, and h are the span length, breadth, and depth of the specimen, respectively. Similarly to the compression bending tests, eight specimens were used for the four-point bending tests.

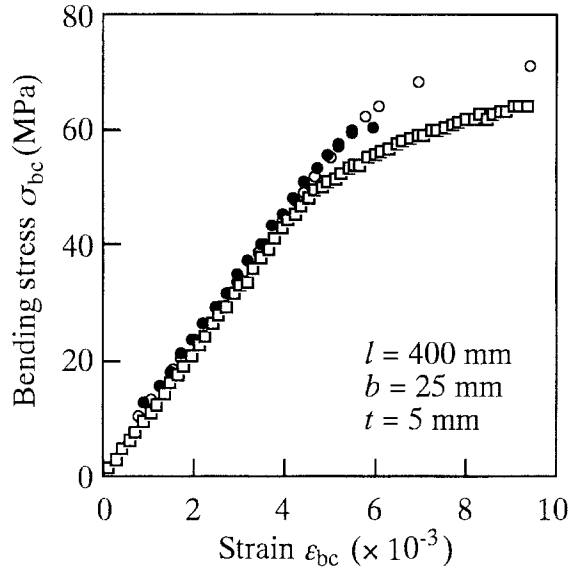

Fig. 8. Example of stress–strain. *Open* and *solid circles*, results obtained from the load–loading point displacement relation and load–strains relation in the compression bending test, respectively. *Squares*, results obtained from the four-point bending test

Results and discussion

Figure 8 shows the stress–strain relations obtained by the compression bending test and the four-point bending test. The shape of the stress–strain relation obtained by the compression bending test was similar to that commonly obtained from the conventional bending test.

Figure 9 shows Young's modulus (E_{bc})corresponding to the length/thickness ratio (l/t). The value of E_{bc} tended to be a constant value, which was a bit larger than that obtained by the four-point bending tests E_{bt} when the length/thickness ratio was large enough. We thought that the additional deflection produced by the shearing force and the stress concentration at the loading point was smaller with the compression bending tests than with the conventional bending tests. Nevertheless, E_{bc} decreased when l/t was less than 20. We thought that this decrease was due to the following two factors. One was material nonlinearity. The smaller the l/t, the larger was the bending stress σ_{bc}. Material nonlinearity, which causes the decrease in stiffness, would be drawn instantly after the bifurcation because of the large bending stress. In addition, when l/t is quite small and the specimen is regarded as an intermediate column, material nonlinearity occurs before bifurcation. The other factor was the additional deflection caused by the shearing force. Although the influence of the shearing force during compression bending is less than with the conventional bending methods, the shearing force that produces the additional deflection cannot be eliminated entirely, and it is marked

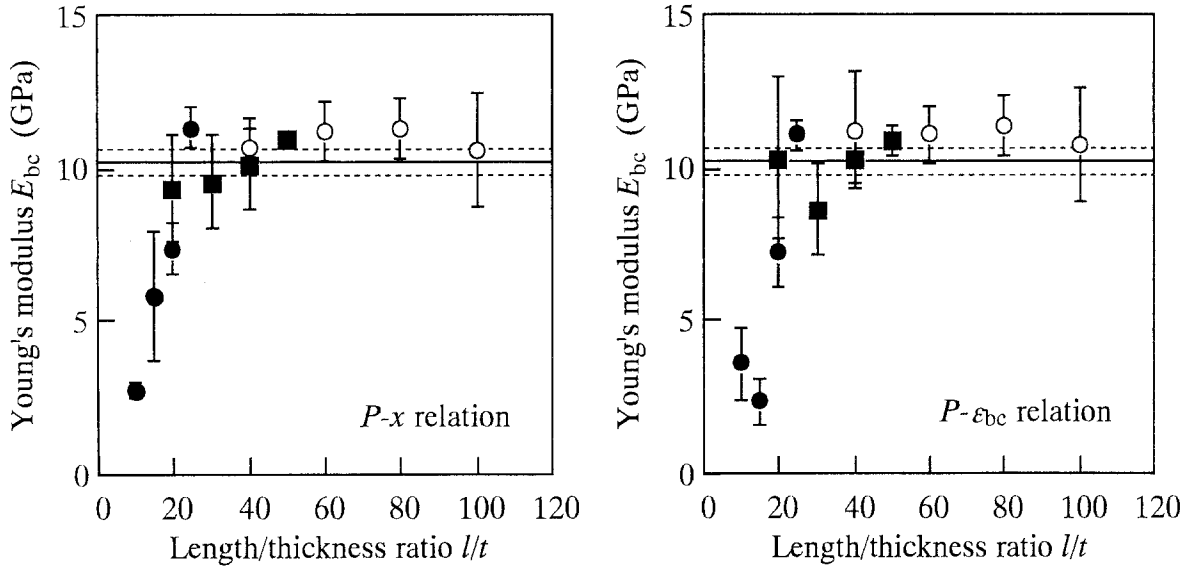

Fig. 9. Young's modulus corresponding to the length/thickness ratio. *Open circles*, *solid squares*, and *solid circles* represent the averages obtained by the compression bending tests of the specimens whose thicknesses were 5, 10, and 20 mm, respectively; *horizontal bars* are the standard deviations obtained by the compression bending tests. *Solid* and *dashed lines* are the average and standard deviations obtained by the four-point bending tests, respectively. P, x, and ε_{bc} are the load, loading point displacement after bifurcation, and strain measured by the gauges, respectively

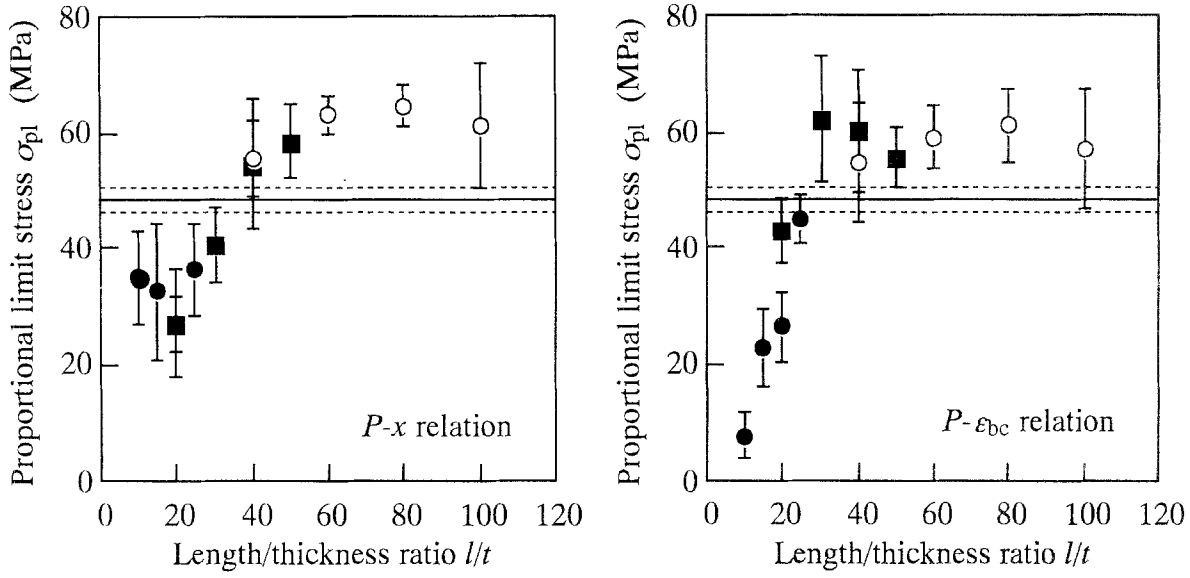

Fig. 10. Proportional limit stress corresponding to the length/thickness ratio. See Fig. 9 for further information

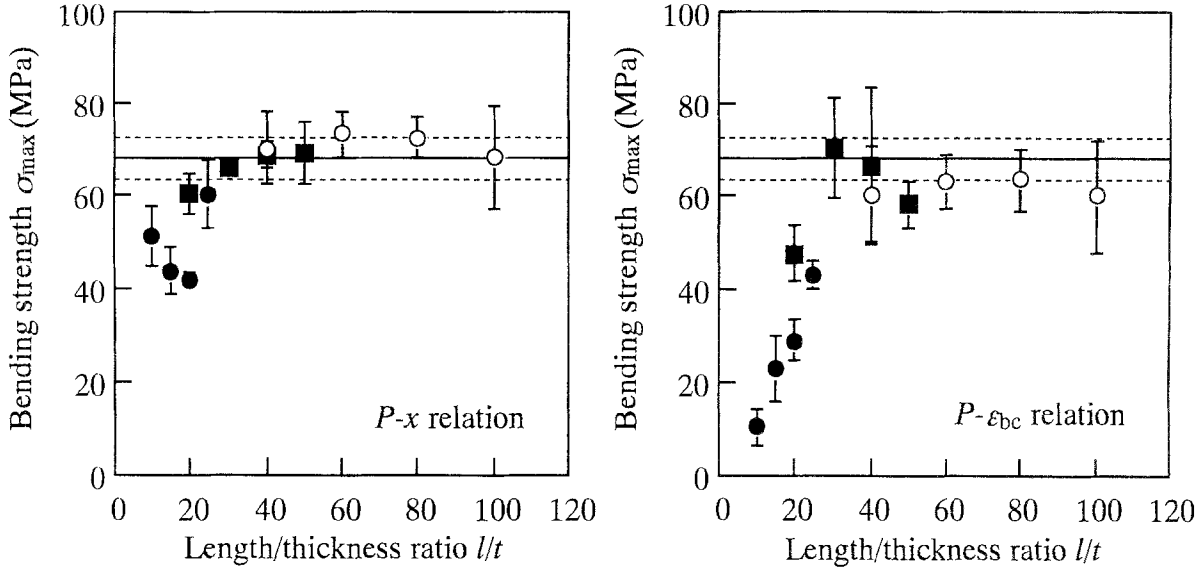

Fig. 11. Bending strength corresponding to the length/thickness ratio. See Fig. 9 for further information

when the l/t is small. To obtain a stable Young's modulus value with the compression bending test, we believe that the length/thickness ratio should be larger than 25.

Figure 10 shows the proportional limit stress σ_{pl} corresponding to the length/thickness ratio l/t. The value of σ_{pl} was constant when the l/t was larger than 40, and it decreased with decreasing l/t. As can be seen from Eq. (17), the proportional limit stress was influenced by Young's modulus, and it showed a tendency similar to that of Young's modulus. However, the value of σ_{pl} exceeded that obtained by the four-point bending tests σ_{bp}, which was more marked in an l/t range larger than 40. We thought that this tendency was due to the absence of stress concentration at the loading points in the compression bending test. In contrast, the stress concentrations, which cause the material nonlinearity and the decrease of proportional limit stress, exist in the four-point bending test. As in Fig. 8, the linear range of the stress–strain relation was larger in the compression bending data than in the four-point bending test data. Based on this result, we think that the compression bending test can be used effectively to determine proportional limit stress without worrying about the influence of the loading point.

Figure 11 shows the bending strength σ_{max} corresponding to the length/thickness ratio l/t. The dependence of the bending strength on the length/thickness ratio shows a similar tendency as Young's modulus and proportional limit stress. However, the bending strength was markedly influ-

enced by the method used to measure strain ε_{bc}. As the deflection increased, the diffusion of wrinkles caused by compressive failure was observed on the compression side of the specimen. These wrinkles caused the unload on the compression side, and the amount of compressive strain ε_c tended to decrease. The radius of curvature at the mid-span ρ was evaluated to be larger from Eq. (8), and the deflection δ calculated by Eq. (14) smaller, than the real value. As shown in Eq. (2), therefore, the bending stress σ_{bc} was evaluated to be smaller because of the low δ value. Therefore, when the deflection is calculated from the strain–strain gauge output, it is feared that the bending strength cannot be measured properly. In contrast to the tendency found with Young's modulus and proportional limit stress, however, the value of σ_{max} in an l/t range larger than 40 was not significantly different from the bending strength obtained from the four-point bending tests σ_{bt}.

For every parameter measured in these experiments, the scatterings in the data obtained by the compression bending tests under the same testing conditions tended to be larger than those obtained by the four-point bending tests. We thought the scatterings were due to the instability of the compression bending method. Despite careful treatment during the compression bending test, the stress–strain relation sometimes cannot be determined because of the eccentrically applied load, the initial curvature of the specimen, and other factors. To obtain a stable relation, these factors should be eliminated as much as possible.

Summarizing these results, we believe that the compression bending test should be conducted on specimens with a large length/thickness ratio (>40 in this experiment) and that the stress–strain relation should be measured by the load–loading point displacement relation for obtaining Young's modulus, proportional limit stress, and bending strength. Under these testing conditions, we would undertake the bending test without worrying about the stress concentration that necessarily occurs with conventional methods. The instability factors in the compression bending test should be reduced carefully as far as possible.

Conclusions

To obtain Young's modulus, proportional limit stress, and bending strength, we conducted the compression bending test on todomatsu columns with various length/thickness ratios. The validity of the testing method was examined by comparing these results with those obtained by conventional four-point bending tests. We concluded that when the stress–strain relation is measured from the load–loading point displacement relation using specimens whose length/thickness ratio is large enough, the bending properties can be obtained by the compression bending test without worrying about the stress concentration that occurs with the conventional methods. The instability factors of the compression bending test should be eliminated as much as possible.

Acknowledgment We thank Prof. Hiroshi Fukuda at the Science University of Tokyo for his advice about conducting the experiment.

References

1. Yoshihara H, Kubojima Y, Nagaoka K, Ohta M (1998) Measurement of the shear modulus of wood by static bending tests. J Wood Sci 44:15–20
2. Yoshihara H, Fukuda A (1998) Influence of loading nose in the static bending test of wood. J Wood Sci 44:473–481
3. Yoshihara H, Matsumoto S (1999) Examination of the proper span/depth ratio range in measuring the bending Young's modulus of wood based on the elementary beam theory. Mokuzai Kogyo 54:269–272
4. Fukuda H (1989) A new bending test method of advanced composites. Exp Mech 29:330–335
5. Fukuda H (1993) Compression bending test method for advanced composites (in Japanese). J Jpn Soc Aerospace Sci 41:482–487
6. Fukuda H, Katoh H, Uesugi H (1995) A modified procedure to measure bending strength and modulus of advanced composites by means of compression bending. J Composite Mater 29:195–207
7. Fukuda H, Itabashi M (1999) Simplified compression bending test method for advanced composites. Composites A 30:249–256
8. Timoshenko SP, Gere JM (1961) Theory of elastic stability. McGraw-Hill, New York, pp 76–82
9. Ramberg W, Osgood WR (1943) Description of stress-strain curves by three parameters. NACA TN-902